Title

Evidence for disrupted gray matter structural connectivity in posttraumatic stress disorder.

Journal

Psychiatry research, 234(2)

ISSN

0165-1781

Authors

Mueller, Susanne G
Ng, Peter
Neylan, Thomas
et al.

Publication Date

2015-11-01

DOI

10.1016/j.pscychresns.2015.09.006

Peer reviewed

Psychiatry Research: Neuroimaging 234 (2015) 194–201

Contents lists available at ScienceDirect

Psychiatry Research: Neuroimaging

journal homepage: www.elsevier.com/locate/psychresns

Evidence for disrupted gray matter structural connectivity in posttraumatic stress disorder

Susanne G. Mueller [a,*], Peter Ng [a], Thomas Neylan [b], Scott Mackin [b], Owen Wolkowitz [b], Synthia Mellon [b], Xiaodan Yan [c], Janine Flory [d], Rachel Yehuda [d], Charles R. Marmar [c], Michael W. Weiner [a]

[a] Center for Imaging of Neurodegenerative Diseases, VAMC San Francisco, Clement Street 4150, San Francisco, CA 94121, USA
[b] Department of Psychiatry, University of California, San Francisco, CA, USA
[c] Department of Psychiatry, NYU School of Medicine, New York, NY, USA
[d] Department of Psychiatry, Icahn School of Medicine at Mount Sinai, New York, NY, USA

ARTICLE INFO

Article history:
Received 27 November 2014
Received in revised form
30 August 2015
Accepted 2 September 2015
Available online 12 September 2015

Keywords:
Posttraumatic stress disorder
Veteran
Graph analysis
Cortical thickness
Structural connectivity

ABSTRACT

Posttraumatic stress disorder (PTSD) is characterized by atrophy within the prefrontal–limbic network. Graph analysis was used to investigate to what degree atrophy in PTSD is associated with impaired structural connectivity within prefrontal limbic network (restricted) and how this affects the integration of the prefrontal limbic network with the rest of the brain (whole-brain). 85 male veterans (45 PTSD neg, 40 PTSD pos) underwent volumetric MRI on a 3T MR. Subfield volumes were obtained using a manual labeling scheme and cortical thickness measurements and subcortical volumes from FreeSurfer. Regression analysis was used to identify regions with volume loss. Graph analytical Toolbox (GAT) was used for graph-analysis. PTSD pos had a thinner rostral anterior cingulate and insular cortex but no hippocampal volume loss. PTSD was characterized by decreased nodal degree (orbitofrontal, anterior cingulate) and clustering coefficients (thalamus) but increased nodal betweenness (insula, orbitofrontal) and a reduced small world index in the whole brain analysis and by orbitofrontal and insular nodes with increased nodal degree, clustering coefficient and nodal betweenness in the restricted analysis. PTSD associated atrophy in the prefrontal–limbic network results in an increased structural connectivity within that network that negatively affected its integration with the rest of the brain.

1. Introduction

Posttraumatic stress disorder (PTSD) is a complex reaction to life threatening or otherwise extremely stressful events that is characterized by re-experiencing symptoms in form of nightmares or flashbacks, states of hyperarousal or numbing and avoidance of trauma related situations and is typically accompanied by poor concentration and difficulty of recalling the details of the traumatic event. Evidence from functional imaging suggests that these symptoms are associated with an impaired interaction between brain regions belonging to the prefrontal–limbic network that is involved in experiencing fear, anxiety and negative emotions (Koenigs and Grafman, 2009). This network encompasses cortical regions particularly mesial and dorsolateral prefrontal and orbitofrontal regions and the insular cortex but also subcortical structures, most importantly amygdala and hippocampus but also thalamus and nucleus (ncl). accumbens regions (Francati et al., 2007; Etkin, 2009; Bremner, 2007; Cisler et al., 2013; Hughes and Shin, 2011). PTSD related abnormalities however are not only functional. Gray matter volume loss or cortical thinning have also been described and are most commonly found in the hippocampus and the mesial prefrontal cortex, particularly anterior cingulate, but occasionally also in the dorsolateral prefrontal and orbitofrontal and insular cortices (Carbo et al., 2005; Geuze et al., 2008; Woon et al., 2010; Karl et al., 2006; Eckart et al., 2011; Kuehn et al., 2011; Rauch et al., 2003; Yamasue et al., 2003), i.e., in the same regions that are affected by the functional disturbances.

Previous studies have shown evidence for a structural morphological connectivity between gray matter structures in the human brain (He and Evans, 2010; Evans, 2013; Alexander-Bloch et al., 2013), i.e., a robust and biologically plausible correlation or covariance between cortical thickness and/or gray matter volumes of anatomically and functionally linked brain areas. Regional cortical thickness or regional gray matter volume are determined by the number and size of neurons and glial cells and the degree of myelination (Carlo and Stevens, 2013; Glasser and Van Essen,

* Corresponding author. Fax: +1 415 668 2864.
E-mail address: susanne.mueller@ucsf.edu (S.G. Mueller).

http://dx.doi.org/10.1016/j.pscychresns.2015.09.006
0925-4927/

2011; Nieuwenhuys et al., 2015). The nature of the covariance of these measures across regions however is not clear and several potential factors, e.g. common afferent/efferent pathways, genetic, maturational/developmental influences, and experience related plasticity alone or in combination have been discussed in this context (Carlo and Stevens, 2013; Evans, 2013; Alexander-Bloch et al., 2013; Chen et al., 2011). Disease processes that alter cortical thickness or gray matter volume however will not only change this normal correlation pattern at the site of the primary insult but also in remote brain regions that interact with this region. In particular, the correlation strength will increase between regions that are either directly and indirectly, e.g., due to loss of input from a directly affected region, affected by the disease process and decrease between affected and non-affected regions. Based on these considerations, the overall goal of this study was to investigate if PTSD related gray matter thinning and/or gray matter volume loss within the prefrontal–limbic network would affect the structural connectivity between those structures and impact their integration into the rest of the brain.

Graph analysis provides a theoretical framework to characterize the connectivity of a network and is increasingly been used to describe the functional and structural connectivity of healthy and diseased brains (Sporns et al., 2000). It describes a network as a system of nodes and edges that connect nodes with similar properties. In terms of in vivo imaging nodes typically represent brain regions for which the property of interest, e.g. cortical thickness, time course of the BOLD signal etc, is known and the edges represent the strength of the correlation between any two regions based on the similarity of this property. The result is a correlation matrix that describes this relationship for every possible combination of regions. In order to obtain a sparse representation of the network and to eliminate edges representing weak and thus most likely irrelevant correlations, this matrix is typically thresholded at a predefined value. Several global and nodal measures can be derived to characterize the remaining connections. For this study the following measures thought to be pertinent to suspected structural pathology in PTSD (Holmes and Wellman, 2009) were chosen. Nodal Measures: a. Degree which is defined as the total number of edges that exist within the network (global degree) or the number of edges that an individual node shares with other nodes (nodal degree). Translated to structural imaging, nodal degree refers to the number of brain regions with which a region of interest shares correlations whose correlation coefficient exceeds the predefined threshold and global degree is the sum of all the pairs of regions that share supra-threshold correlations. A node representing a brain region with atrophy is more likely to have correlations exceeding the threshold and thus share edges with other nodes representing brain regions that affected by the same disease process than with nodes representing regions that are spared by the disease process (cf Supplementary Fig. and comment). b. The clustering coefficient represents the fraction of all possible connections that connect the neighbors of a given node. Although neighborhood in graph analysis refers to topological distance in the network, this often also implies anatomical neighborhood in brain structural networks based on gray matter volumes/thickness. A high clustering coefficient associated with thinning in the node or region of interest therefore indicates that the thinning extends at least to some degree to the anatomical neighbors of that region. c. Nodal betweenness centrality is defined as the fraction of all shortest paths that pass through an individual node. The path length is defined as the minimum number of unique edges connecting two nodes and thus a high nodal betweenness centrality indicates that this node is connected to many other nodes that are only one or two edges away. In healthy brains nodal betweeness centrality is therefore considered to be a measure of the importance of a node in the network. In brains with focal gray matter atrophy however, nodal betweenness centrality will also be increased in nodes in atrophied regions because the atrophy will strengthen the correlation between the region of interest with anatomically neighboring regions affected by atrophy but weaken those between the region of interest and remote regions without atrophy. Global Measures: a. Characteristic path length (lambda) is defined as the average of all nodal paths and global clustering coefficient (gamma) as the average of all nodal clustering coefficient. b. A network is considered to have a small world topology if it is characterized by a high mean clustering coefficient but relatively short characteristic path length. Small world topology is considered to represent a particularly economical network configuration because it supports segregated/specialized and distributed/integrated information processing equally well (Sporns et al., 2000; Bassett Smith and Bullmore, 2006; 2009). Disease processes impairing the structural integrity due to gray matter atrophy/thinning result in a less economical network structure and thus in a lower small world index at the whole brain network level. c. Global betweenness centrality is defined as the average of the nodal betweenness.

Based on the findings of previous volumetric studies (Karl et al., 2006), we expected to find the most prominent PTSD related gray matter volume losses in the hippocampus (restricted to subfields CA1 and dentate gyrus (McEwan, 2001) and the most prominent cortical thinning in the mesial prefrontal cortex (anterior cingulate, mesial superior frontal lobe region). Given the fact that the atrophied structures of the limbic–prefrontal network are tightly interconnected, we expected PTSD to be associated with increased structural connectivity between structures of the prefrontal–limbic network. It is important to keep in mind that the increased connectivity is associated with various degrees of atrophy within the prefrontal–limbic structures, i.e., it indicates a disruption of the prefrontal limbic network. The consequence of this local disruption, is an impaired integration of prefrontal limbic network with the non-atrophied structures of the remaining brain. Specifically we expected 1. to find signs of an increased connectivity, i.e., increased nodal degree, clustering coefficients and nodal betweenness centrality in PTSD pos compared to PTSD neg, when restricting the analysis to the limbic–prefrontal network. This atrophy was expected to increase the connectivity within the limbic–prefrontal network but to impair their interaction with non-atrophied regions/nodes outside the prefrontal network. Consequently, we expected 2. nodal degree and clustering coefficient of the limbic prefrontal nodes to be decreased in PTSD pos when analyzed within the whole brain network. The nodal betweenness centrality of the nodes in regions with atrophy though was expected to be increased in the whole brain network analysis as well due to a disproportionate loss of long and intermediate paths connecting the prefrontal–limbic region with non-atrophied regions outside compared to the mostly maintained short paths connecting it with other regions in the prefrontal–limbic network. Finally it was expected that the changes at the regional level translate into a decreased small world index as evidence for less efficient structural brain organization in PTSD at the global level.

2. Methods

2.1. Study sample

The sample consisted of 85 male veterans who had participated in Operation Iraqi Freedom (OIF) and/or Operation Enduring Freedom (OEF). They represent a subset of the first 100 subjects who were recruited for a Department of Defense sponsored multisite project that is aiming to identify reliable PTSD markers using a combination of clinical, genetic, endocrine, multi-omic and

imaging information. The participants were recruited by advertising from the community and from three clinical centers (NYU School of Medicine, James J. Peters VA Medical Center and Mount Sinai School of Medicine). The inclusion criteria for this study were: 1. Male combat exposed US OIF/OEF veteran. 2. Between 20 and 60 years of age. 3. Positive for OIF/OEF warzone related PTSD (at least 3 months duration, Clinician Administered PTSD Scale (CAPS) > 40) or negative for PTSD (CAPS < 20, negative for lifetime PTSD). 4. Written consent stating the ability to understand the study procedures and the willingness to participate in the study. Exclusion criteria were. 1. Current or recent non OIF/OEF related trauma. 2. History of open head injury or closed head injury with loss of consciousness of more than 10 min to exclude participants with a history of moderate-severe concussion. 2. Current or past neurological or systematic disorders affecting CNS function. 3. Current or past (within last 12 months) alcohol or drug abuse/dependence. The 12 month period was chosen to ensure that the past abuse did not influence any of blood or urine markers investigated in this study.. 4. History of psychiatric disorder with psychotic features, bipolar disorder or obsessive–compulsive disorder. 5. Suicidal or homicidal ideation. 6. Change of medical regimen less than 2 months before the screening. Of the 100 recruited subjects, 15 had to be excluded from the study because of insufficient imaging data quality and so the final study sample consisted of 40 PTSD positive veterans (PTSD pos) and 45 PTSD negative veterans (PTSD neg). The Committees of Human Research of all participating institutions had seen and approved of the study protocol (cf. Table 1 for demographic and clinical information).

2.2. Imaging

All subjects were studied on a 3 T Trio Siemens magnet (Erlangen, Germany) at NYU equipped with a 32 channel receive head coil. The following sequences that were part of a larger research imaging protocol were obtained: 1) T1-weighted 3D whole brain gradient echo MRI TR/TE/TI = 2300/2.98/900 ms, $1.0 \times 1.0 \times 1.0$ mm^3 resolution (cortical thickness measurements). 2. T2 weighted 3D whole brain spin echo MRI TR/TE 3200/422 ms, $1.0 \times 1.0 \times 1.0$ mm^3 resolution (intracranial volume (ICV) estimation) 3) high resolution T2 weighted fast spin echo sequence for hippocampal subfield volumetry (TR/TE: 4120/43 ms, 0.4×0.4 mm^2 in plane resolution, 2 mm slice thickness, 24 interleaved slices, angulated perpendicular to the long axis of the hippocampal formation (hippocampal subfield volumetry).

Table 1
Demographic and clinical information.

	PTSD negative	PTSD positive
No	45	40
Age	33.6 (8.4) range: 22–58	32.7 (7.7) range: 23–53
Smokers	6	15
CAPS Current	2.96 (4.37)	67.2 (17.7)*
CAPS_Lifetime	9.07 (7.88)	89.85 (15.50)*
BDI	5.42 (6.18)	25.70 (10.60)*
BDI > 18	2	34
Psychotrop Med	2	9
ETISR	5.60 (4.20)	6.78 (4.86)
PCL	25.22 (8.26)	59.22 (10.87)*

BDI, Beck's Depression Index; ETISR, Early Trauma Inventory Self-Report; PCL, PTSD Checklist Total Score.
Smokers: more than 100 cigarettes over lifetime in cigarette use questionaire.
Psychotrop Med; current treatment with psychotropic medication.
* $p < 0.05$ Wilcoxon test.

2.3. Cortical thickness measurement

FreeSurfer (version 5.1, https://surfer.nmr.mgh.harvard.edu) was used for cortical surface reconstruction and cortical thickness estimation. The procedure has been extensively described elsewhere (Fischl and Dale, 2000; Fischl et al., 2004a, 2004b; Dale et al., 1999; Desikan et al. 2006). In short, the Freesurfer processing stream consists of the co-registration of the subject T1 image to an atlas for bias correction and intensity normalization, brain extraction/removal of non brain tissue, initial tessellation and refinement of the gray/white matter boundary (white surface) followed by an outward nudging of the resulting surface using the intensity gradients between gray matter and CSF (pial surface). The resulting surfaces are inflated and co-registered to a probabilistic template to label cortical areas. The subcortical structures are labeled by co-registering the subject brain to a probabilistic labeled template in Talairach space. The transformation matrices are then inverted to project the labels from the template space into the subject space and to obtain regional volumetric and thickness information. A trained rater visually checked the final FreeSurfer outputs (cortical and subcortical labels, thickness measurements) for accuracy or processing failures in a systematic and standardized manner and applied edits/corrections when necessary. The results of this quality control were logged in a database. Only data that had a full pass, i.e. the cortical and subcortical labels and thickness measurements captured all subcortical structures and the gray matter rim in all lobes correctly, was used in this study. FreeSurfer volumes used for volumetric analyses were corrected for differences of ICV using the following formula (Raz et al., 2005): Adjusted volume = raw volume $- b \times$ (ICV − mean ICV) where b is the slope of the regression of a volume on ICV. Since there was no a priori hypothesis regarding lateralization of the abnormalities, the volumes/thickness measures of both sides were combined by summing them up. The following brain regions were considered to belong to the prefrontal–limbic network: entorhinal cortex, hippocampal subfields CA1, CA3&dentate gyrus (cf. next paragraph), ncl. accumbens, amygdala, thalamus, rostral and caudal anterior cingulate cortices, superior frontal lobe cortex, rostral and caudal dorsolateral frontal cortices, lateral and medial orbitofrontal cortices and insula.

2.4. Hippocampal subfield volumetry

The method used for subfield marking including assessment of measurement reliability has been described in detail previously (Mueller et al., 2007, 2010). In brief, the marking scheme depends on anatomical landmarks, particularly on a hypointense line representing myelinated fibers in the stratum moleculare/lacunosum which can be reliably visualized on these high resolution images. Together with external landmarks, e.g. fimbria, collateral sulcus etc. this line is used to identify and manually label the subiculum, the cornu ammonis sectors CA1-CA3 and the dentate gyrus on a length of about 1 cm in the anterior third of hippocampal body. The labeling section is restricted to the anterior section for the sake of efficiency (ca. 60–90 min/subject for an experienced rater) and because the hippocampal tail is not always completely covered with 24 slices. Correction for differences of ICV was done with the same formula as used for the FreeSurfer volumes. The subfield volumes of both sides were combined.

2.5. Graph analysis

The Graph-Analysis-Toolbox 1.3.2. (GAT) (http://ncnl.stanford.edu/tools.html) running under Matlab 2012b (Hadi Hosseini et al., 2012 was used for graph analysis. GAT uses the routines in the Brain Connectivity Toolbox (BCT, https://sites.google.com/site/bctnet/) to extract network measures from the binary adjacency

matrices at a global and regional level. The raw (not corrected for head size) left and right subiculum, CA1, CA3&dentate gyrus volumes from the high resolution image, and the volumes from the left and right amygdala, accumbens, thalamus and all regional cortical thickness measures from FreeSurfer (total 80 regions or nodes) were combined for these analyses. The validity of combining the data from the two sequences had been established in previous publications (Mueller et al., 2010, 2012; Raj et al., 2010). The combined volume and thickness data was used to calculate a whole brain and a prefrontal limbic Pearson correlation matrix for each of the two groups. These matrices were thresholded at minimal density (density = fraction of connections/edges present in the network compared to the maximal possible number of connections/edges; minimal density = density below which the networks are no longer fully connected or density at which each node within the network shares at least one edge with one other node) and converted into binary adjacency maps. The minimal density threshold was chosen to allow for a meaningful comparison of the graph analytical measures between the whole brain network and the network restricted to prefrontal–limbic structures because it ensured that all nodes of interest were included in both networks. Hundred null networks that preserved the topology, e.g., number of nodes, total edges of the original data, were constructed for each group network to assess their small world characteristics. Similarly as the original networks, they were thresholded at minimal density and converted into binary adjacency matrices. The key metrics determining small world topology are the mean clustering coefficient C and the mean characteristic path length L over all nodes. A small world network is characterized by a larger mean clustering coefficient than that seen in random networks with similar topology, i.e. gamma = Cnet/Cran > 1, but about the same path length, i.e. lambda = Lnet/Lran ~ 1. A scalar summary of small-worldness (sigma) is therefore the ratio between gamma/lambda which is typically > 1 (Achard et al., 2006). The network properties were assessed at the whole brain level with all nodes (80 regions, 'whole brain network') and in a network limited to the a priori regions (28 regions, 'prefrontal–limbic network').

2.6. Statistical analysis

Volumetric data: The Kolomogorov–Smirnov test that was used to test the imaging and demographic data for normal distribution indicated a skewed distribution for age that was corrected by log transformation. Furthermore, the descriptive data analysis showed an uneven distribution of Hispanics vs non Hispanics (Fisher's exact test, $p < 0.001$) between the two groups with a higher percentage of Hispanics in the PTSD pos group (53.9% pos vs 31.8% neg) and a higher percentage of Non-Hispanics in the PTSD neg group (46.2% pos vs 68.2%) and thus ethnicity was included in the statistical model. Multiple linear regression analyses with volume/thickness as dependent and group (PTSD pos, PTSD neg), age and ethnicity as independent variables were used to test for PTSD effects in the prefrontal–limbic network (a priori regions) and in the rest of the brain (non a priori cortical regions). False discovery rate (FDR) $p < 0.05$ was used to correct for multiple comparisons in the non a priori regions.

Graph-analysis: A one-sided non-parametric permutation test (1000 repetitions) was used to test for the global and regional differences of the network measures between the two groups as specified in the hypotheses. The minimal density thresholds are recalculated for each repetition. FDR $p < 0.05$ was used to correct for multiple comparisons in the non a priori regions (52 regions) at the regional level.

Table 2
ICV corrected A priori mean (SD) subfield and subcortical volumes.

	PTSD negative	PTSD positive
ERC	128.5 (21.4)	132.1 (25.6)
Sub	105.1 (17.1)	110.3 (18.9)
CA1	384.0 (41.5)	384.0 (42.1)
CA1-2 transition	20.9 (24.3)	17.5 (29.5)
CA3&DG	266.0 (43.6)	255.2 (37.9)
Hippocampus	8704.9 (641.6)	8562.7 (647.1)
Amygdala	3507.4 (312.0)	3523.0 (37
Ncl. accumbens	1271.9 (155.5)	1217.6 (178.9)
Thalamus	16340.7 (1148.3)	16424.5 (1188.4)

Left and right side are combined, volumes are given in mm^3.
(SD) standard deviation, ERC entorhinal cortex.
CA, cornu amonis sectors;DG, dentate gyrus;Ncl, nucleus.

Table 3
Mean (SD) cortical thickness measurements of A priori regions.

	PTSD negative	PTSD positive
Rostral anterior cingulate	5.76 (0.32)	5.60 (0.37)*
Caudal anterior cngulate	5.12 (0.38)	5.03 (0.35)
Superior frontal	5.51 (0.21)	5.45 (0.18)
Rostral mid frontal	4.74 (0.19)	4.74 (0.16)
Caudal mid frontal	5.20 (0.19)	5.13 (0.20)
Medial orbitofrontal	4.87 (0.20)	4.83 (0.25)
Lateral orbitofrontal	5.30 (0.22)	5.20 (0.29)
Insula	6.2 (0.24)	6.10 (0.32)*

Left and right side are combined, thickness in mm.
(SD) standard deviation.
* $p < 0.05$ compared to PTSD neg.

3. Results

Tables 2 and 3 provide an overview over the volume/thickness differences between PTSD pos and PTSD neg in the a priori regions. PSTD associated cortical thinning was found in the posterior cingulate, precentral and transverse temporal region in the post hoc analyses but these differences were no longer significant after FDR correction (Table 4)

Prefrontal–limbic network: The minimal density threshold was 0.1825 (r threshold: PTSD neg: 0.3992; PTSD pos: 0.4426). PTSD neg did not differ from PTSD pos regarding global efficiency (0.320 vs 0.346), global clustering (0.532 vs 0.521) and mean node betweenness (0.827 vs 1.528). Nodal degree, cluster coefficient and betweenness centrality were significantly increased in the orbitofrontal region and insula, please see Fig. 1 for details.

Whole brain network: The minimal density threshold was 0.2066 (r threshold: PTSD neg: 0.4223; PTSD pos: 0.4893) in the whole brain analysis. The small world index sigma was significantly higher in PTSD neg compared to PTSD pos (1.311 vs 0.869, $p = 0.007$). PTSD neg did not differ from PTSD pos regarding global efficiency (0.444 vs 0.496), global clustering (0.555 vs 0.548) and mean node betweenness (53.725 vs 89.375). Significant decreases of nodal degree and/or cluster coefficient and nodal betweenness centrality were found in nodes of the orbitofrontal, cingulate and insula region and in the thalamus, please see Fig. 1 for details.

4. Discussion

There were three findings that will be discussed in more detail in the following sections: 1. In contrast to our hypothesis, there was no PTSD associated global or regional (subfield) hippocampal

Table 4
Mean (SD) cortical thickness measurements of non A priori regions.

	PTSD negative	PTSD positive
Posterior cingulate	5.14 (0.25)	5.01 (0.25)
Isthmus cingulate	5.09 (0.40)	4.96 (0.34)
Pars orbitalis	5.49 (0.29)	5.40 (0.40)
Pars opercularis	5.30 (0.22)	5.31 (0.25)
Pars triangularis	5.04 (0.20)	5.10 (0.25)
Precentral	5.18 (0.21)	5.07 (0.24)
Frontal pole	5.54 (0.40)	5.54 (0.38)
Temporal multimod ass cortex	5.32 (0.22)	5.29 (0.28)
Parahippocampus	5.58 (0.42)	5.68 (0.46)
Fusiform	5.67 (0.21)	5.58 (0.26)
Inferior temporal	5.86 (0.23)	5.80 (0.30)
Middle temporal	6.05 (0.24)	6.02 (0.26)
Superior temporal	5.87 (0.24)	5.82 (0.35)
Transverse temporal	4.97 (0.30)	4.78 (0.35)
Temporal pole	7.40 (0.46)	7.34 (0.55)
Paracentral	4.83 (0.22)	4.75 (0.21)
Postcentral	4.32 (0.23)	4.30 (0.22)
Precuneus	4.97 (0.20)	4.93 (0.03)
Superior parietal	4.62 (0.20)	4.63 (0.21)
Inferior parietal	5.15 (0.18)	5.16 (0.21)
Lingual	4.18 (0.22)	4.15 (0.21)
Supramarginal	5.24 (0.20)	5.25 (0.25)
Lateral occipital	4.62 (0.20)	4.65 (0.26)
Cuneus	3.89 (0.22)	3.87 (0.23)
Pericalcarine	3.44 (0.25)	3.40 (0.23)

Left and right side are combined, thickness in mm.
(SD) standard deviation.
Multimod, multimodal; Ass, association.

volume loss. However, PTSD was associated with cortical thinning in the rostral anterior cingulate and the insula as has been shown by previous studies. 2. Although the structural abnormalities were regionally confined, they were associated with changes throughout the prefrontal–limbic network that are consistent with an increased structural connectivity within this network (increased nodal degree, nodal betweenness and clustering coefficient). 3. The structural changes within the prefrontal–limbic network negatively affected its integration into the rest of the brain (loss of efficient connections as evidenced by a decreased nodal degree and clustering connectivity, increased nodal betweenness) which resulted in a less organized and efficient global structural connectivity and loss of small world organization in PTSD. Taken together, these findings demonstrate that the well documented disturbances of the prefrontal–limbic functional connectivity in PTSD have structural correlates.

The first finding of this study meriting further discussion was that PTSD was associated with thinning of the rostral anterior cingulate and insular cortices but not with hippocampal volume loss. The former finding is consistent with the findings of many previous studies investigating structural abnormalities in PTSD (Karl et al., 2006) but the latter is somewhat surprising because hippocampal volume loss is one of the most consistently reported findings in PTSD (Woon et al., 2010). In contrast to most previous studies, this study not only obtained a global hippocampal volume (hippocampus label from Freesurfer) but also regional subfield specific volumes (manual labeling) but neither approach showed a significant volume loss. Voxel-based morphometry that was performed to rule out regional volume losses that might not be detectable by the other two approaches, e.g. volume loss restricted to the hippocampal tail, (data not shown) also confirmed the absence of significant hippocampal volume losses in this sample. It seems therefore unlikely that technical issues e.g., limited coverage of the hippocampus by the manual labeling scheme, caused the absence of hippocampal volume loss in this study, but indicates that it is a true negative finding. There are several potential explanations for the lack of hippocampal volume loss in this study. For example, the participants of this study were all veterans of the OIF/OEF conflicts and about 10-25 years younger compared to other studies in veterans that reported PTSD associated hippocampal volume losses in which most were Vietnam and/or Gulf War veterans (Chao et al., 2013; Wang et al., 2010). Since hippocampal neurogenesis declines with age (Burger, 2010; McEwen, 2002), it is possible that the effect of PTSD on the hippocampus was mitigated by a more efficient neurogenesis in this younger sample or that the volume losses in older veterans were exaggerated by hippocampal volume loss due to concurrent incipient neurodegenerative diseases, e.g. vascular lesions or Alzheimer's disease. Other possible explanations include non-accounted for genetic factors (Bayer et al., 2013; Braune et al., 2012; Palombo et al., 2013) or environmental/occupational hazards. For example, in contrast to other studies both PTSD pos and PTSD neg participants were combat-exposed veterans, and so it could be possible that the experience of combat itself (Gong et al., 2014) or a combat related event, e.g., mild traumatic brain injury due to blast exposure (Monti et al., 2013), could have had a negative impact on the hippocampus and diminished the PTSD related effect. At this point all these potential explanations are highly speculative and need to be further investigated. The conclusion that can be drawn however is that although a PTSD related hippocapmpal volume loss is common, it is not always present. This suggests that it will be necessary to better understand the factors influencing hippocampal size in PTSD and to take this knowledge into account if the hippocampal volume or hippocampal subfield volume are to be used as an imaging biomarker for PTSD.

The second finding meriting further discussion was the demonstration of a disrupted structural connectivity in PTSD. In addition to the quite extensive literature reporting PTSD related changes in task-related fMRI studies (for example, Bruce et al., 2012; Sripada et al., 2013; Kilgore et al., 2014; Stevens et al., 2013), there are now also several publications that demonstrate alterations of the functional connectivity in task free fMRI (**for example**, Jin et al., 2013; Brown et al., 2013; Li et al., 2013; Xie et al., 2013; Rabinak et al., 2011). The existence of a functional disruption is thus well documented. However, to our knowledge the current study is one of the first to show a disruption of the structural connectivity. Typically DTI and fiber tracking together with graph analysis is used to assess structural connectivity and this was also the approach used by Long et al. (2013) which to our knowledge is the only other study that investigated structural connectivity with graph analysis in PTSD to date. This group compared 17 patients suffering from PTSD about 8 months after a motor vehicle accident with 15 healthy controls and found evidence for an altered nodal betweenness and efficiency mostly in prefrontal nodes but also extending into nodes in the temporal/temporal-limbic regions. Despite those extensive regional abnormalities, the small world topology was maintained. Graph analysis in conjunction with cortical thickness or gray matter volumes as was done in this study has been used to investigate structural connectivity in healthy subjects and normal aging and in a variety of disease states e.g., Alzheimer's disease, epilepsy, multiple sclerosis (He et al., 2007, 2008, 2009; Bernhardt et al., 2011; Hadi Hosseini et al., 2012; Fahim et al., 2011) but to our knowledge this is the first study to do this in PTSD. The goal of the current study was to investigate local as well as remote effects of PTSD on structural connectivity. For the former, the graph analysis was restricted to the brain regions belonging to the prefrontal–limbic network, for the latter the interaction of prefrontal–limbic structures with rest of the brain was investigated by performing a whole brain graph analysis. The findings within the prefrontal limbic network show significantly increased nodal degree, clustering coefficients and nodal betweenness in regions with (insula) and without (orbitofrontal) atrophy which can be interpreted as evidence for an

Prefrontal-limbic network

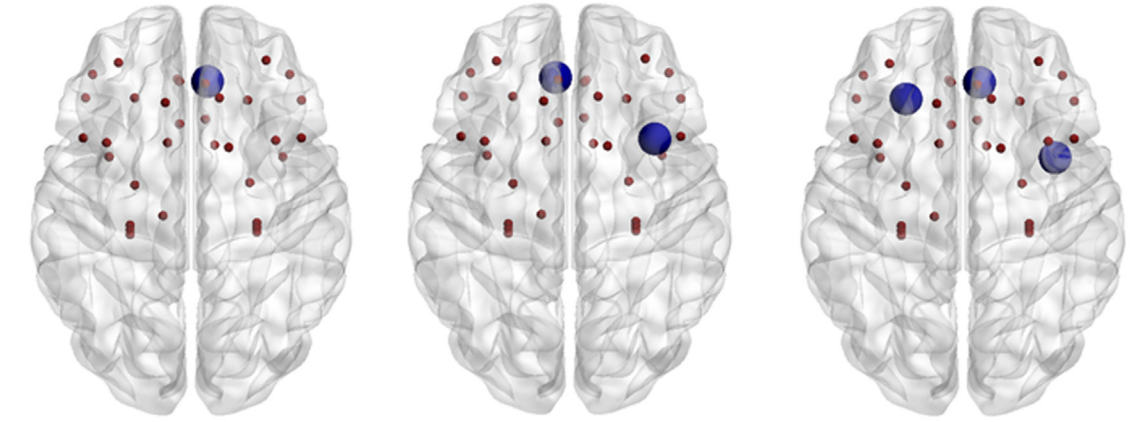

Measure	Region	PTSD neg	PTSD pos
Degree	R MedialOrbitofrontal	2	8

Measure	Region	PTSD neg	PTSD pos
Cluster Coeff	L MedialOrbitofrontal	0.53	1
	R LateralOrbitofrontal	0.36	0.64

Measure	Region	PTSD neg	PTSD pos
Nodal Betw	L LateralOrbitofrontal	5.49	167.45
	R MedialOrbitofrontal	0.00	48.14
	R Insula	5.40	93.95

Whole brain network

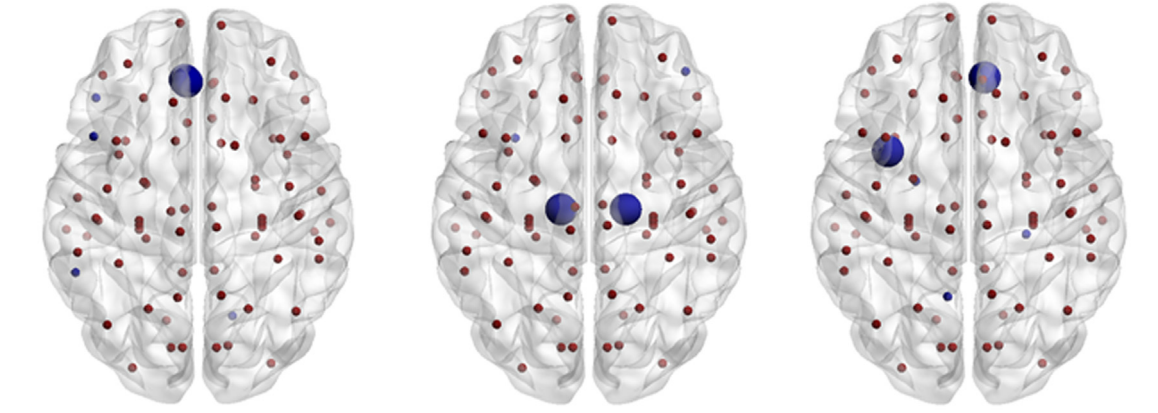

Measure	Region	PTSD neg	PTSD pos
Degree	L MedialOrbitofrontal	29	9
	L RostralAnteriorCingulate	18	2
	L Bankssts	*36*	*13*
	L ParsOpercularis	*34*	*14*
	L ParsTriangularis	*34*	*8*
	R Lingual	*23*	*7*

Measure	Region	PTSD neg	PTSD pos
Cluster Coeff	L Thalamus	1	0
	R Thalamus	1	0
	L TemporalPole	*1*	*0*
	R ParsOrbitalis	*0.92*	*0.59*

Measure	Region	PTSD neg	PTSD pos
Nodal Betw	L Insula	60.7	447.4
	R MedialOrbitofrontal	0.0	184.5
	L entorhinal	*0.0*	*294.7*
	L Precuneus	*61.4*	*672.4*
	R Parahippocampal	*130.3*	*544.9*

Fig. 1. Findings of regional graph analysis. Top row, prefrontal–limbic network (restricted network). Blue, nodes with significant increases of degree, cluster coefficient (cluster coeff) and nodal betweenness centrality (nod Betw) in PTSD pos compared to PTSD neg. Lower row, regional findings in whole brain network. Large blue nodes, significant regional decreases (degree, cluster coefficient (cluster coeff) and increases (nodal betweenness centrality (nod Betw) within the a priori region/prefrontal–limbic region, small blue nodes significant findings within non a priori regions. Region names in italic, regions in the non a priori regions with significant changes that became non-significant after FDR correction. (For interpretation of the references to color in this figure legend, the reader is referred to the web version of this article.)

increased connectivity between prefrontal limbic structures. In a whole brain network analysis without atrophy the term increased connectivity usually indicates a more efficient network structure. In this case however, the increased connectivity was associated with a more or less pronounced gray matter volume loss/thinning, i.e., pathological process mostly restricted to this particular network and thus has to be interpreted as pathological process resulting in a less efficient network structure at the whole brain network level. The assumption of an impaired prefrontal limbic function is supported by the findings of a recent study (Yan et al., 2013) that investigated intrinsic spontaneous activity in the same group of OIF/OEF veterans with task free fMRI and found also an increased spontaneous activity in the insula and orbitofrontal cortex but in addition to that also in the amygdala and anterior cingulate. The increased structural connectivity between structures within the prefrontal–limbic network impairs its interaction with the remainder of the brain as is demonstrated by the findings of the whole brain analysis. In the whole brain analysis, the regional or nodal connectivity measures of the prefrontal–limbic network are determined by influences from within and outside the prefrontal–limbic network. In the context of the local findings, the finding of decreased nodal degree and clustering coefficients in orbitofrontal, anterior cingulate, insula and thalamus in the whole brain analysis can thus be interpreted as evidence for a reduced

interaction of these regions with structures outside the prefrontal–limbic network. This is also supported by the increased nodal betweenness within some of these structures which in the context of the other changes can be interpreted as evidence for an enhanced connectivity within the prefrontal network but loss of efficient connections with other brain regions. At the global level finally, all these changes translate into a loss of the small world organization in PTSD.

The study has limitations. 1. In contrast to task-free fMRI based functional connectivity and DTI/tractography based structural connectivity which are based on individual correlation matrices, structural connectivity based on gray matter volumes/thickness requires the calculation of group correlation matrices. It is therefore not possible to investigate to what degree individual subjects show the changes seen at the group level nor to study the effect of continuous variables on these structural abnormalities. 2. As explained in the methods section, this study used the minimal density threshold to allow for an easily interpretable comparison of the graph analytical measures between the whole brain network and the prefrontal–limbic sub-network. Previous studies investigating whole brain structural connectivity based on gray matter thickness/volumes typically used a higher threshold or range of higher thresholds that result in more sparse networks and consequently different graph analytical measures. This is best evidenced in the small world index found in this study that with 1.311 and 0.869 was lower than those reported in sparser networks. Using a density threshold of 0.1 would have resulted in small world indices of 1.605 and 1.356 ($p=$ns). This makes a direct comparison of our findings with other studies more difficult. 3. The PTSD plus group had higher BDI scores than the PTSD neg group. Including BDI in the statistical model did not change the findings in the volumetric analyses. Nonetheless, we cannot exclude that depression contributed to the findings.

In conclusion, the findings of this study show that even relatively circumscribed gray matter thinning results in a widespread disturbance of the structural connectivity in PTSD. This suggests that the well known functional abnormalities that have been described within the prefrontal limbic network have at least in this sample a structural correlate. This finding will need to be confirmed when the data of the second half of the participants is ready be analyzed.

Acknowledgment

This work has been supported by the U.S. Department of Defense: Grants W81XWH-09-2-0044 and W81XWH-10-1-0021.

Appendix A. Supplementary material

Supplementary data associated with this article can be found in the online version at http://dx.doi.org/10.1016/j.pscychresns.2015.09.006.

References

Achard, S., Salvador, R., Whitcher, B., Suckling, J., Bullomore, E., 2006. A resilient, low-frequency, small-world human brain functional network with highly connected association cortical hubs. J. Neurosci. 26, 63–72.

Alexander-Bloch, A., Raznahan, A., Bullmore, E., Giedd, J., 2013. The convergence of maturational change and structural covariance in human cortical networks. J. Neurosci. 33, 2889–2899.

Bassett Smith, D., Bullmore, E., 2006. Small-world networks. Neuroscientist 12, 512–523.

Basett, D.S., Bullmore, E.T., 2009. Human brain networks in health and disease. Curr. Opin. Neurol. 22, 340–347.

Bayer, J., Rune, G., Kutsche, K., Schwarze, U., Kalisch, R., Buechel, C., Sommer, T., 2013. Estrogen and the male hippocampus: genetic variation in aromatase gene predicting serum estrogen is associated with hippocampal gray matter volume in men. Hippocampus 23, 117–121.

Bernhardt, B.C., Chen, Z., He, Y., Evans, A.C., Bernasconi, N., 2011. Graph-theoretical analysis reveals disrupted small-world organization of cortical thickness correlation networks in temporal lobe epilepsy. Cereb. Cortex 21, 2147–2157.

Braune, B.T., Konrad, C., Grotegard, D., Suslow, T., Ohrmann, P., Bauer, J., Arolt, V., Heindel, W., Domschke, K., Schoening, S., Rauch, A.V., Sehlmeyer, P., Kugel, H., Dannlowski, U., 2012. Tumor necrosis factor gene variation predicts hippocampal volume in healthy individuals. Biol. Psychiatry 72, 655–682.

Bremner, J.D., 2007. Neuroimaging in posttraumatic stress disorder and other stress-related disorders. Neuroimaging Clin. N 17, 523.

Brown, V.M., Labar, K.S., Haswell, C.C., Gold, A.L., Mid-Atlantic MIRECCWorkgroup, Beall, S.K., Van Voorhees, Marx, E., Calhoun, C.E., Fairbank, P.S., Green, J.A., Tupler, K.T., Weiner, L.A., Beckham, R.D., Brancu, J.C., Hoerle, M., Pender, J.M., Kudler, M., Swinkels, H., Nieuwsma, C.M., Runnals, J.A., Youssef, J.J., McDonald, N.A., Davison, S.D., Yoash-Gantz, R., Tabler, R., Hurley, K.H., McCarthy, R., Morey, G., 2013. Altered-resting state functional connectivity of basolateral and centromedial amygdala complexes in posttraumatic stress disorder. Neuropsychopharmacology, 351–359. http://dx.doi.org/10.1038/npp.2013.197.

Bruce, S.E., Buchholz, K.R., Brown, W.J., Yan, L., Durbin, A., Sheline, Y.I., 2012. Altered emotional interference processing in the amygdala and insula in women with post-traumatic stress disorder. Neuroimage 2, 43–49.

Burger, C., 2010. Region-specific genetic alterations in the aging hippocampus: implications for cognitive aging. Front. Aging Neurosci. 2, 140. http://dx.doi.org/10.3389/fnagi.2010.00140.

Carbo, V., Clement, M.H., Armony, J.L., Pruessner, J.C., Brunet, A., 2005. Size versus shape differences: Contrasting voxel-based and volumetric analysis of the anterior cingulate cortex in individuals with acute posttraumatic stress disorder. Biol. Psychiatry 58, 119–124.

Carlo, C.N., Stevens, C.F., 2013. Structural uniformity of neocortex, revisited. Proc. Natl. Acad. Sci. 110, 1488–1493.

Chao, L., Weiner, M., Neylan, T., 2013. Regional cerebral volumes in veterans with current versus remitted postraumatic stress disorder. Psychiatry Res. 213, 193–201.

Chen, C.H., Panizzon, M.S., Eyler, L.T., Jernigan, T.L., Thompson, W., Fenneman – Notestine, C., Jak, A.J., Neale, M.C., Franz, C.E., Hamza, S., Lyons, M.J., Grant, M.D., Fischl, B., Seidman, L.J., Tsuang, M.T., Kremen, W.S., Dale, A.M., 2011. Genetic influence on cortical regionalization in human brain. Neuron 72, 537–544.

Cisler, J.M., Steele, J.S., Lenow, J.K., Smitherman, S., Everett, B., Messias, E., Kilts, C.D., 2013. Unctional reorganization of neuronal networks during repeated exposure to the traumatic memory in posttraumatic stress disorder: an exploratory fMRI study. J. Psychiatry Res. 3956, 00305–00311. http://dx.doi.org/10.1016/j.jpsychires.2013.09.013.

Dale, A.M., Fischl, B., Sereno, M.I., 1999. Cortical surface-based analysis I: segmentation and surface reconstruction. Neuroimage 9, 179–194.

Desikan, R.S., Ségonne, F., Fischl, B., Quinn, B.T., Dickerson, B.C., Blacker, D., Buckner, R.L., Dale, A.M., Maguire, R.P., Hyman, B.T., Albert, M.S., Killiany, R.J., 2006. An automated labeling system for subdividing the human cerebral cortex on MRI scans into gyral based regions of interest. Neuroimage 31, 968–980.

Eckart, C., Stoppel, C., Kaufmann, J., Tempelmann, C., Hinrichs, H., Elbert, T., Heinze, H.J., Kolassa, I.T., 2011. Structural alterations in latera; prefrontal, parietal and posterior midline regions of men with chronic posttraumatic stress disorder. J. Psychiatry Neurosci. 36, 176–186.

Etkin, A., 2009. Functional neuroanatomy of anxiety: a neural circuit perspective. In: Stein, M.B., Steckler, T. (Eds.), Behavioral Neurobiology of Anxiety and its Treatment. Current Topic in Behavioral Neurosciences. Springer Verlag, Berlin, Heidelberg.

Fahim, C., He, Y., Yoon, U., Chen, J., Evans, A., Pérusse, D., 2011. Neuroanatomy of childhood disruptive behavior disorders. Aggress. Behav. 37, 326–337.

Evans, A.,C., 2013. Networks of anatomical co-variance. Neuroimage 80, 489–504.

Francati, V., Vermetten, E., Bremner, J.D., 2007. Functional neuroimaging studies in posttraumatic stress disorder: review of current methods and findings. Depression Anxiety 24, 202–218.

Fischl, B., Dale, A.M., 2000. Measuring the thickness of the human cerebral cortex from magnetic resonance images. Proc. Natl. Acad. Sci. USA 97, 11050–11055.

Fischl, B., Salat, D.H., van der Kouwe, A.J., Makris, N., Ségonne, F., Quinn, B.T., Dale, A. M., 2004a. Sequence-independent segmentation of magnetic resonance images. Neuroimage 23 (Suppl. 1), S69–S84.

Fischl, B., van der Kouwe, A., Destrieux, C., Halgren, E., Ségonne, F., Salat, D.H., Busa, E., Seidman, L.J., Goldstein, J., Kennedy, D., Caviness, V., Makris, N., Rosen, B., Dale, A.M., 2004b. Automatically parcellating the human cerebral cortex. Cereb. Cortex 1, 11–22.

Glasser, M.F., Van Essen, D.C., 2011. Mapping human cortical areas in vivo based on myelin content revealed by T1 and T2 weighted MRI. J. Neurosci. 31, 11597–11616.

Geuze, E., Westenberg, H.G.M., Heinecke, A., de Kloet, C.S., Goebel, R., Vermetten, E., 2008. Thinner prefrontal cortex in veterans with posttraumatic stress disorder. Neuroimage 41, 675–681.

Gong, Q., Li, L., Tognin, S., Wu, Q., Pettersson –Yeo, W., Lui, S., Huang, X., Marquand, A.F., Mechelli, A., 2014. Using structural neuroanatomy to identify trauma survivors with and without post-traumatic stress disorder at the individual level. Psychol. Med. 44 (1), 195–203. http://dx.doi.org/10.1017/S0033291713000561.

Hughes, K.C., Shin, L.M., 2011. Functional neuroimaging studies of post-traumatic stress disorder. Expert Rev. Neurother. 11 (2), 275–285. http://dx.doi.org/

10.1586/ern.10.198.
Hadi Hosseini, S.M., Hoeft, F., Kesler, S.R., 2012. GAT: A graph-theoretical analysis toolbox for analysing between-group differences in large scale structural and functional brain networks. PLOS One 7, e40709. http://dx.doi.org/10.137/1/journal.pone.0040709.
He, Y., Chen, Z.J., Evans, A.C., 2007. Small-world anatomical networks in the human brain revealed by cortical thickness from MRI. Cereb. Cortex 10, 2407–2419.
He, Y., Chen, Z., Evans, A., 2008. Structural insights into aberrant topological patterns of large-scale cortical networks in Alzheimer's disease. J. Neurosci. 28, 4756–4766.
He, Y., Dagher, A., Chen, Z., Charil, A., Zijdenbos, A., Worsley, K., Evans, A., 2009. Impaired small-world efficiency in structural cortical networks in multiple sclerosis associated with white matter lesion load. Brain 132, 3366–3379.
He, Y., Evans, A., 2010. Graph theoretical modeling of brain connectivity. Curr. Opin. Neurol. 23, 341.
Holmes, A., Wellman, C.L., 2009. Stress induced prefrontal reorganization and executive dysfunction in rodents. Neurosci. Behav. Rev. 33, 773–783.
Jin, C., Qi, R., Yin, Y., Hu, X., Duan, L., Xu, Q., Zhang, Z., Zhong, Y., Feng, B., Xiang, H., Gong, Q., Liu, Y., Lu, G., Li, L., 2013. Abnormalities in whole brain functional connectivity observed in treatment naïve post-traumatic stress disorder patients following an earthquake. Psychol. Med. 29, 1–10.
Karl, A., Schaefer, M., Malta, L.S., Doerfel, D., Rohleder, N., Werner, A., 2006. A meta-analysis of structural brain abnormalities in PTSD. Neurosci. Behav. Rev. 30, 1004–1031.
Kilgore, W.D., Britton, J.C., Schwab, Z.J., Price, L.M., Weiner, M.R., Gold, A.L., Rosso, I. M., Simon, N.M., Pollack, H.M., Rauch, S.L., 2014. Cortico-limbic responses to masked affective faces across PTSD, panic disorder and specific phobia. Depress. Anxiety 31 (2), 150–159. http://dx.doi.org/10.1002/da.22156.
Koenigs, M., Grafman, J., 2009. Posttraumatic stress disorder: The role of the medial prefrontal cortex and amygdala. Neuroscientist 15, 540–548.
Kuehn, S., Schubert, F., Gallinat, J., 2011. Structural correlates of traint anxiety: reduced thickness in medial orbitofrontal cortes accompanied by volume increase in nucleus accumbens. J. Affect. Disord. 134, 315–319.
Li, X., Zhu, D., Jiang, X., Jin, C., Zhang, X., Guo, L., Zhang, J., Hu, X., Li, L., Liu, T., 2013. Dynamic functional connectonomics signatures for characterization and differentiation of PTSD patients. Hum. Brain Mapp. 14. http://dx.doi.org/10.1002/hbm.22290, May.
Long, Z., Duan, X., Xie, B., Du, H., Li, R., Xu, Q., Wei, L., Zhang, S.X., Wu, Y., Gao, Q., Chen, H., 2013. Altered brain structural connectivity in post-traumatic stress disorder: a diffusion tensor imaging tractography study. J. Affect. Disord. 150, 798–806.
McEwan, B.S., 2001. Plasticity of the hippocampus: adaptation to chronic stress and allosteric load. Ann. N.Y. Acad. Sci. 933, 265–277.
McEwen, B.S., 2002. Sex, stress and the hippocampus: allostasis, allostatic load and the aging process. Neurobiol. Aging 25, 921–939.
Monti, J.M., Voss, M.W., Pence, A., McAuley, E., Kramer, A.F., Cohen, N.J., 2013. History of mild traumatic brain injury is associated with deficits in relational memory, reduced hippocampal volume, and less neural activity later in life. Front. Aging Neurosci. 5, 41. http://dx.doi.org/10.3389/fnagi.2013.00041.
Mueller, S.G., Stables, L., Du, A.T., Schuff, N., Truran, D., Cashdollar, N., Weiner, M.W., 2007. Measurement of hippocampal subfields and age-related changes with high resolution MRI at 4T. Neurobiol. Aging 28, 19–25.
Mueller, S.G., Schuff, N., Yaffe, K., Madison, C., Miller, B., Weiner, M.W., 2010. Hippocampal atrophy patterns in mild cognitive impairment and Alzheimer's Disease. Hum. Brain Mapp. 31, 1339–1347.
Mueller, S.G., Laxer, K.D., Scanlon, C., Garcia, P., McMullen, W.J., Meador, K.J., Weiner, M.W., 2012. Different structural correlates for verbal memory impairment in temporal lobe epilepsy with and without mesial temporal lobe sclerosis. Hum. Brain Mapp. 33, 489–499.
Mueller, S.G., Laxer, K.D., Barakos, J., Cheong, I., Finlay, D., Garcia, P., Cardenas-Nicolson, V., Weiner, M.W., 2010. Involvement of the thalamocortical network in TLE with and without mesio-temporal sclerosis. Epilepsia 51, 1528 1167.
Nieuwenhuys, R., Broere, C.A.J., Cerliani, L., 2015. A new myeloarchitectonic map of the human neocortex based on data from the Vogt–Vogt school. Brain Struct. Funct. 220 (5), 2551–2573. http://dx.doi.org/10.1007/s00429-014-0806-9.
Palombo, D.J., Amaral, R.S., Olsen, R.K., Mueller, D.J., Todd, E.M., Anderson, A.K., Levine, B., 2013. KIBRA polymorphism is associated with individual differences in hippocampal subregions: evidence from anatomical segmentation using high resolution MRI. J. Neurosci. 33, 13088–13093.
Rabinak, C.A., Angstadt, M., Welsh, R.C., Kennedy, A.E., Lyubkin, M., Martis, B., Phan, K.L., 2011. Altered amygdala resting-state functional connectivity in posttraumatic stress disorder. Front. Psychiatry 2, 62. http://dx.doi.org/10.3389/fpsych2011.00062.
Raj, A., Mueller, S.G., Young, K., Laxer, K.D., Weiner, M.W., 2010. Network-level analysis of cortical thickness of the epileptic brain. Neuroimage 52, 1302–1313.
Rauch, S.L., Shin, L.M., Segal, E., Pitman, R.K., Carson, M.A., McMullin, K., Whalen, P. J., Makris, N., 2003. Selectively reduced regional cortical volumes in posttraumatic stress disorder. Neuroreport 14, 913 196.
Raz, N., Lindenberger, U., Rodrique, K.M., Kennedy, K.M., Head, D., Williamson, A., Dahle, C., Gerstorf, D., Acker, J.D., 2005. Regional brain changes in aging healthy adults: general trends, individual differences and modifiers. Cereb. Cortex 15, 1676–1689.
Sporns, O., Tononi, G., Edelman, G.M., 2000. Theoretical neuroanatomy: relating anatomical and functional connectivity in graphs and cortical connection matrices. Cereb. Cortex 10, 127–141.
Sripada, R.K., Garfinkel, S.N., Liberzon, I., 2013. Avoidant symptoms in PTSD predict fear circuit activation during multimodal fear extinction. Front. Hum. Neurosci. 7, 672. http://dx.doi.org/10.3389/fnhum.2013.00672.
Stevens, J.S., Jovanovic, T., Fani, N., Ely, T.D., Glover, E.M., Bradley, B., Ressler, K.J., 2013. Disrupted amygdala-prefrontal functional connectivity in civilian women with posttraumatic stress disorder. Journal of Psychiatry Research 47, 1469–1478.
Wang, Z., Neylan, T., Mueller, S.G., Lenoci, M., Truran, D., Marmar, C.R., Weiner, M. W., Schuff, N., 2010. Magnetic resonance imaging of the hippocampal subfields in posttraumatic stress disorder. Arch. Gen. Psychiatry 67, 296–303.
Woon, F.L., Sood, S., Hedges, D.W., 2010. Hippocampal volume deficitis associated with exposure to psychological trauma and posttraumatic stress disorder in adults: a meta-analysis. Prog. Neuro-Psychopharmacol. Biol. Psychiatry 34, 1181–1188.
Xie, B., Qiu, M.G., Zhang, Y., Zhang, J.N., Li, M., Chen, H., Zhang, Y., Zhang, J.J., Wang, J., Chen, W., Du, H.J., Zhang, S.X., 2013. Alterations in the cortical thickness and the amplitude of low-frequency fluctuation in patients with post-traumatic stress disorder. Brain Res. 1490, 225–232.
Yamasue, H., Kasai, K., Iwanami, A., Othani, T., Yamada, H., Abe, O., Kuroki, N., Tochigi, M., Furukawa, S., Sadamatsu, M., Sasaki, T., Aoki, S., Othomo, K., Asukai, N., Kato, N., 2003. Voxel-based analysis of MRI reveals anterior cingulated gray-matter volume reduction in posttraumatic stress disorder due to terrorism. Proc. Natl. Acad. Sci. 100, 9039–9043.
Yan, X., Brown, A.D., Lazar, M., Cressman, V.L., Henn-Haase, C., Neylan, T., Shalev, A., Wolkowitz, O.M., Hamilton, S., Yehuda, R., Sodickson, D.K., Marmar, C.R., 2013. Spontaneous brain activity in combat related PTSD. Neurosci. Lett. 547, 1–5.